Cross talk between bistable elements on an InSb étalon

James Young, Harvey Richardson, Hugh A. MacKenzie, and Eitan Abraham

Department of Physics, Heriot-Watt University, Edinburgh, UK

David J. Hagan

Center for Research in Electro-optics and Lasers, Department of Physics, University of Central Florida, Orlando, Florida 32816-0001

Received May 13, 1987; accepted September 17, 1987

Cross talk due to transverse carrier diffusion between identical bistable elements on an InSb étalon at 80 K is studied both theoretically and experimentally. Measurements of cross talk between two such elements show that typically, for a practical system, a critical separation of a few diffusion lengths between beam centers is necessary for independent operation. When the difference between holding and switching powers approaches zero, the results show that the critical distance diverges. Delays as great as 4 μsec have been observed when one element is switched and its neighbor is induced to switch through the cross-talk mechanism. These delays can be partially attributed to critical slowing down, and, in principle, they diverge as the interelement distance is increased toward the critical separation. A theoretical model based on the diffusion equation for the single-pass nonlinear phase shift shows how the critical separation depends on physical parameters and the number of elements forming an array. We found that the relevant interaction is essentially limited to nearest neighbors. When the theory is applied to two bistable elements, good agreement is obtained with the experiments in both the steady and the dynamic states.

1. INTRODUCTION

The advent of logic elements based on optical bistability has advanced the possibility of all-optical computing systems. The demonstration of a three-element loop circuit[1] has established the basic format for the serial processing of optically encoded data. A fundamental limit to the achievable serial data rate is the switching speed of the individual bistable elements. However, higher data rates may be developed by using parallel processing. This processing would take the form of an optical array in which all the elements would be involved in the simultaneous but independent handling of information. This method raises a question about packing densities since the minimum separation of elements will in practice be limited by the extent of the transverse coupling between them. This coupling, or cross talk, is not necessarily confined to adjacent elements, but it can be a long-range effect, as in thermal nonlinearities in interference filters[2,3]—with severe consequences on interelement separation necessary for channel isolation.

The object of this paper is to address some of these questions. We report measurements of, and a theoretical model on, transverse-diffusive coupling between two bistable elements on an InSb étalon. The dependence of critical distance (d_{crit}) on the holding power is investigated. (d_{crit} is defined[2] as the smallest separation by which an element can sustain itself in the OFF state while the other element is in the ON state.) In addition, we investigate the temporal dependence of the switching process through controlled cross talk by choosing the separation.

The diffusion of photoexcited carriers in InSb has been studied[4] by the angular dependence of degenerate four-wave mixing. The results indicated that the carrier-diffusion length l_D is ~60 μm in one recombination time. The theoretical model presented here is based on carrier diffusion as the sole transverse coupling mechanism. This is a short-range effect when compared with thermal diffusion; hence spacing of only a few diffusion lengths is necessary for independent operation of adjacent elements. Furthermore, the theory predicts that for any number of elements forming a two-dimensional array only nearest neighbors influence d_{crit}. The critical separation diverges as the holding power approaches the switch point.

In this paper we present a systematic study of the dynamics of cross talk between adjacent bistable channels in an InSb étalon and develop a theory to analyze the geometric aspects and the time dependence of the effects. The implications for all-optical data processing are also considered.

2. EXPERIMENT

The experimental layout is shown in Fig. 1. Two beams, A and B, incident upon the étalon of InSb ($n \simeq 10^{14}$ cm^{-3}) were produced from the same cw CO laser operating at a frequency of $\bar{\nu}$ = 1819 cm^{-1}. Each beam could be independently controlled in incident power and position on the 280-μm-thick étalon held at 80 K in a liquid-nitrogen reservoir cryostat. The beams were linearly polarized at 90° with respect to each other, which allowed discrimination of the two output beams and minimized any optical interference effects.

The procedure to establish d_{crit} involved setting up two identical, adjacent bistable channels, A and B, in the étalon. This task was achieved by adjusting beam A with lens L_3 to give optimum beam radius[5] and minimum switching power. Beam B was then adjusted independently, using lens L_2, so that with beam A blocked, channel B gave identical switching characteristics. An area of 100 μm × 1500 μm was found on the étalon, over which the switching power was constant to ±2%, and the cross-talk experiment was confined to this region.

The incident plane of the étalon was imaged into a thermal camera by using lens L_4, and the channel spacing was

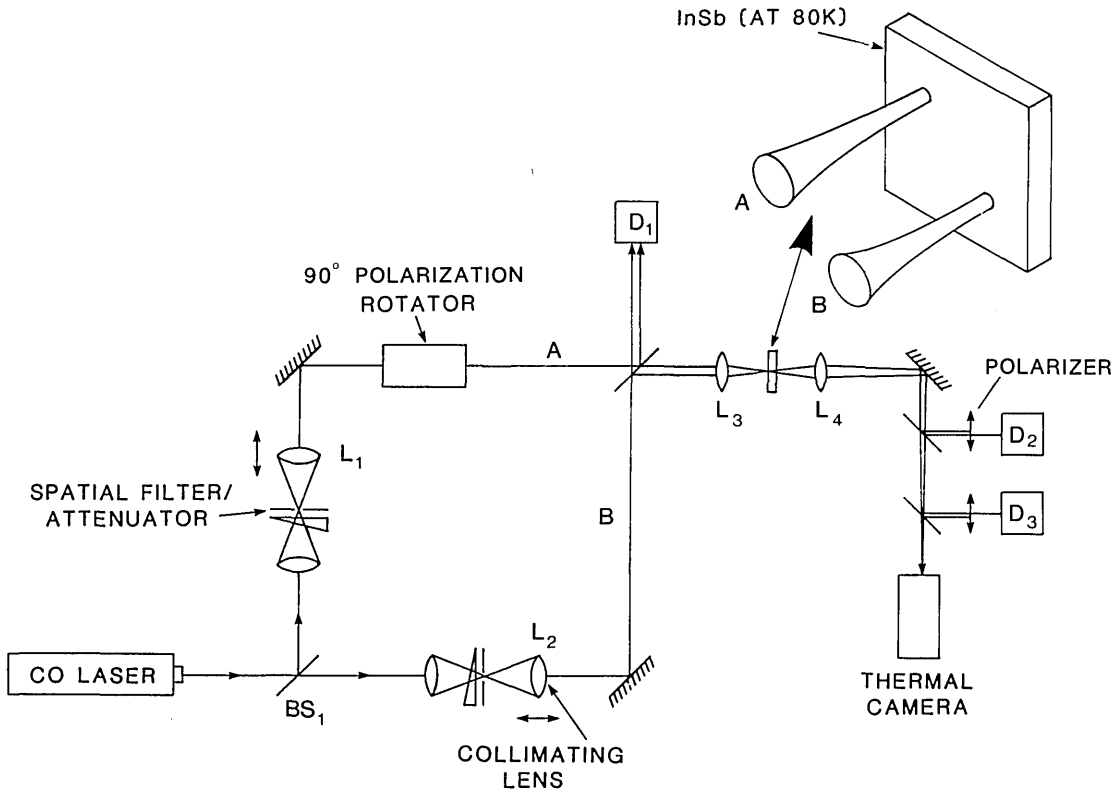

Fig. 1. Schematic of experimental setup: L's, lenses; BS_1, beam splitter. Both inputs were detected by detector D_1; individual outputs were detected by detectors D_2 and D_3.

measured on a monitor screen. The imaging system was calibrated with a precision pinhole of known diameter. In a typical experimental run, beams A and B were set at a chosen separation with identical holding beam powers with the standoff from switching, ΔP, determined by

$$\Delta P = (1 - P_{\mathrm{hold}}/P_s)100,$$

where P_{hold} is the holding power and P_s is the single-element switch power. When beam A was switched to the ON state and after a certain time delay, beam B would spontaneously switch on if there were sufficient transfer of carriers between the channels. Both the channel spacing and the standoff from switching could be varied, and, for a particular setting of ΔP, the channel spacing could be increased until transfer of switching ceased. This experimental determination of d_{crit} is summarized in Fig. 2. The time delay involved in the transfer of switching is illustrated in Fig. 3(a), and the composite results are summarized in Fig. 3(c), where switch delay times are plotted as a function of ΔP for three values of interelement spacing. For small values of ΔP (<2%), the

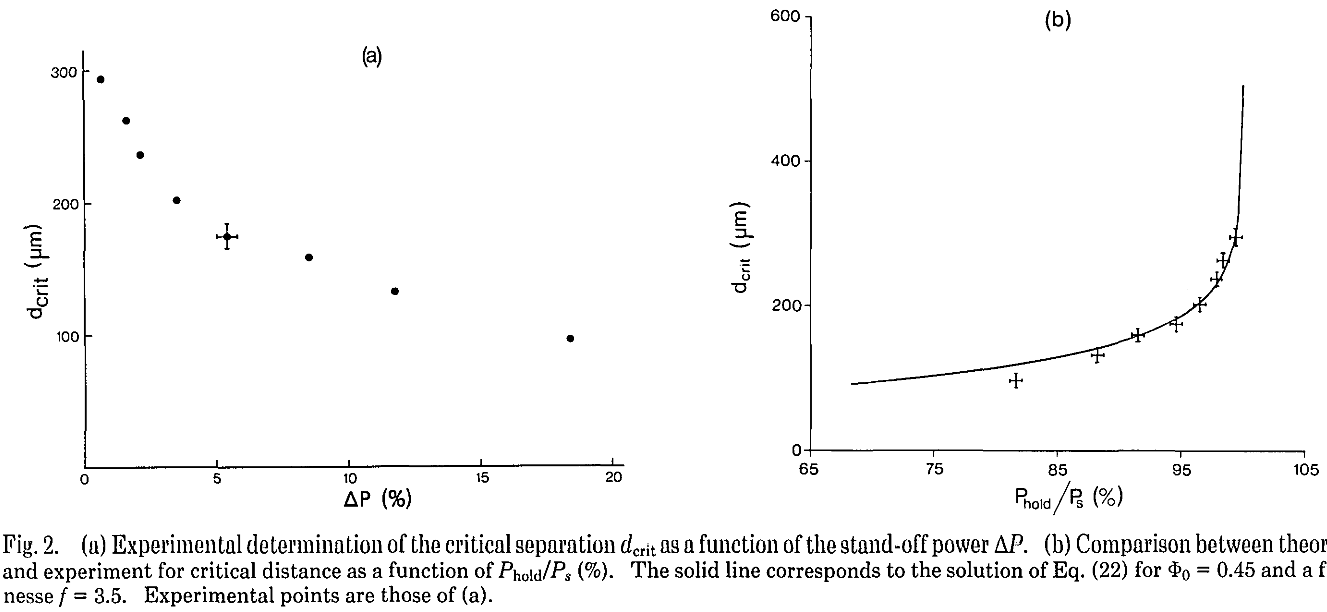

Fig. 2. (a) Experimental determination of the critical separation d_{crit} as a function of the stand-off power ΔP. (b) Comparison between theory and experiment for critical distance as a function of P_{hold}/P_s (%). The solid line corresponds to the solution of Eq. (22) for $\Phi_0 = 0.45$ and a finesse $f = 3.5$. Experimental points are those of (a).

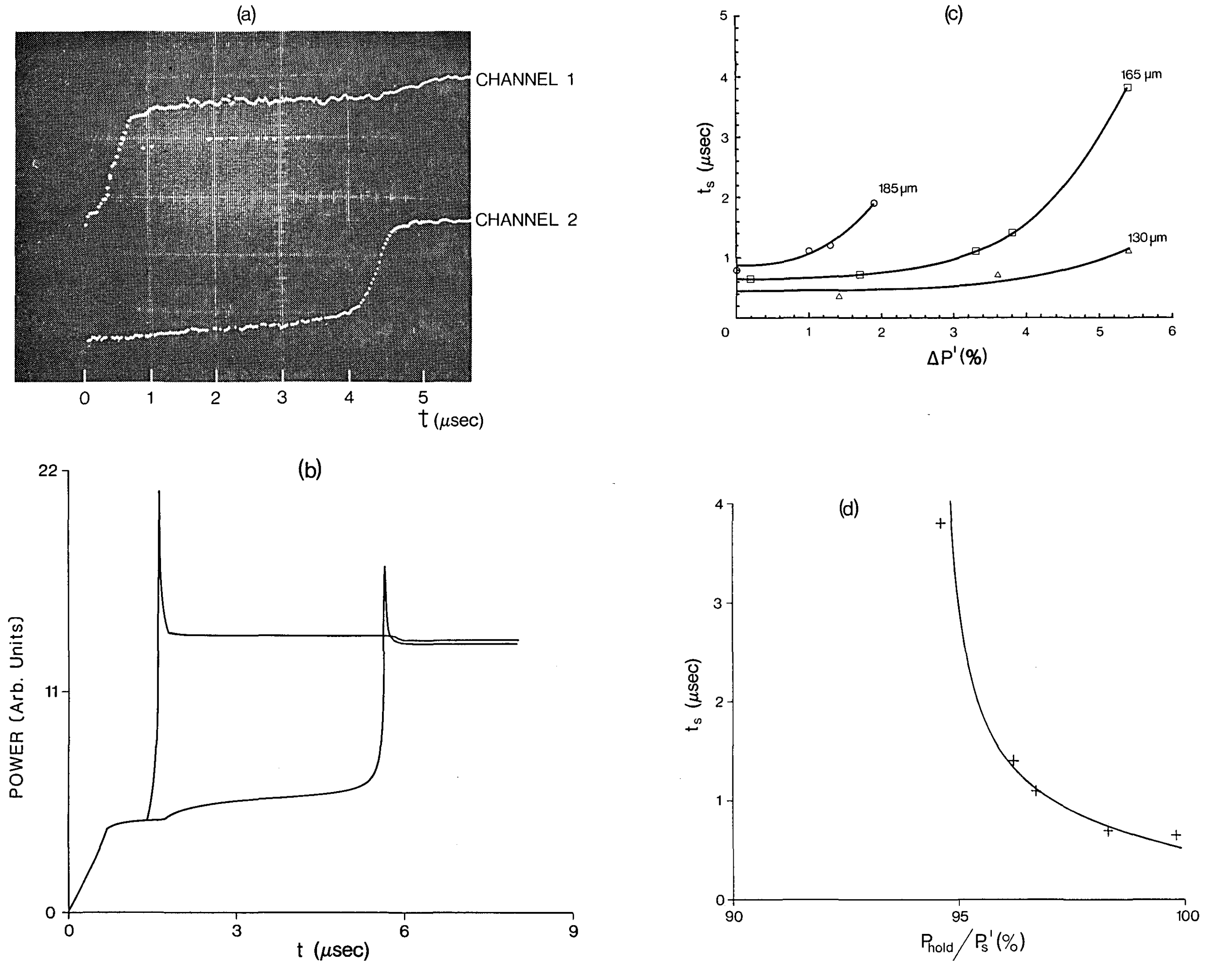

Fig. 3. (a) Oscilloscope trace of the time evolution of the transmitted powers showing the delay between the switching of channel 1 (E1) and channel 2 (E2) for $d = 165\ \mu m$ and $\Delta P' \equiv (1 - P_{hold}/P_s')100 = 5.2\%$, where $P_s' \propto I_s'$ (see Section 3). Here $d_{crit} \simeq 180\ \mu m$. (b) Numerical simulation of (a) for the transmitted powers by solving Eq. (14). Note that the sharp overshooting is the result of calculating at beam centers: parameters, $f = 3.5$, $\Phi_0 = 0$. (c) Experimental plot of the time delay versus ΔP for various separations. (d) Switching times as in (c) but in terms of P_{hold}/P_s' (%). Note that P_s' changes with separation. Solid line corresponds to theory for $\Phi_0 = 1.8$ and $w = 0.5 l_D$.

time delay is simply the transit time for carriers to diffuse from element A to B, but at larger values of ΔP, where the transfer of switching becomes more marginal, the switching process is subject to critical slowing-down effects, and microsecond delays are observed. The implications of these results are discussed in Section 4.

3. THEORY

In this section the theory is developed by starting with an outline of the general equations from which the derivation[6,7] of the diffusion equation for the single-pass nonlinear phase shift Φ is obtained. By using the appropriate Green function, a system of integral equations for Φ at each beam center, in both the time-dependent and steady states, is derived. Then critical separations and their dependence on detuning, finesse, and spot radius are calculated.

Consider a nonlinear medium in a Fabry–Perot resonator of mirror reflectivities R_F (front) and R_B (back) where light propagates in the z direction. We assume that the local refractive index is given by $n = n_0 + n_2 I_c$, where I_c is the internal intensity, and that the cavity round-trip time is $\tau_r \ll \tau$ (recombination time). Then, after adiabatic elimination of the field variables and in the limit of strong diffusion, we can write

$$\partial F(\mathbf{r}, z, t)/\partial z = [-(\alpha L/2) + iN(\mathbf{r}, z, t) + i(\mathcal{F}/2)\nabla_T^2]F(\mathbf{r}, z, t), \quad (1)$$

$$-\partial B(\mathbf{r}, z, t)/\partial z = [-(\alpha L/2) + iN(\mathbf{r}, z, t) + i(\mathcal{F}/2)\nabla_T^2]B(\mathbf{r}, z, t), \quad (2)$$

$$l_T^2\nabla_T^2 N(\mathbf{r}, z, t) + l_L^2\partial^2 N(\mathbf{r}, z, t)/\partial z^2 - \tau\partial N(\mathbf{r}, z, t)/\partial t - N(\mathbf{r}, z, t) = -4\mathcal{F}\,\mathrm{sgn}(n_2)(|F(\mathbf{r}, z, t)|^2 + |B(\mathbf{r}, z, t)|^2), \quad (3)$$

where

$$\begin{bmatrix} F \\ B \end{bmatrix} = (n_0 c/16P_c)^{1/2}\begin{bmatrix} E_f \\ E_b \end{bmatrix}$$

are the scaled forward and backward electric field envelopes, c is the speed of light, $P_c = \lambda^2/2\pi n_0|n_2|$ is the critical power for self-focusing, $\mathcal{F} = \lambda L/2\pi n_0 w^2$ is the Fresnel number, L is the cavity length, w is the spot radius, $\nabla_T^2 = \partial^2/\partial x^2 + \partial^2/\partial y^2$ is the transverse Laplacian scaled to w^2, N is the excitation density, z is scaled to L, $l_T \equiv l_D/w$, $l_L \equiv l_D/L$, and $l_D = (D\tau)^{1/2}$, and D is the diffusivity.

Equations (1)–(3) can be derived from the Maxwell–Bloch equations in the limit of high dispersion[8] where the excitation density is a scaled population inversion. Unless $l_D \gg \lambda$ we should also include population-grating terms (standing-wave effects), which double the phase shift imposed on the counterpropagating fields by each other (nonlinear nonreciprocity). In this section an InSb étalon in which N is the photogenerated-carrier concentration is considered.

The boundary conditions of this problem are

$$F(\mathbf{r}, o, t) = (1 - R_F)^{1/2}F_{\text{in}}(\mathbf{r}, t) + R_F^{1/2}B(\mathbf{r}, o, t)\exp(-2i\Phi_0), \quad (4)$$

$$B(\mathbf{r}, 1, t) = R_B^{1/2}F(\mathbf{r}, 1), \quad (5)$$

$$N(\mathbf{r}, z, t) \to 0 \quad \text{as } |\mathbf{r}| \to \infty, \quad (6)$$

$$(l_T^2/\tau)\partial N(\mathbf{r}, p, t)/\partial z = N(\mathbf{r}, p, t)S \quad (p = 0, 1), \quad (7)$$

where Φ_0 is the linear cavity detuning and S is the surface-recombination velocity. In the present experimental conditions we can neglect diffraction in Eqs. (1) and (2) since for $L = 280\ \mu$m and $\lambda = 5.5\ \mu$m we get an effective diffraction area $\lambda L = 1540\ \mu\text{m}^2$ smaller than l_D^2 ($\sim 3600\ \mu\text{m}^2$). Then, defining the single-pass nonlinear phase shift

$$\Phi(\mathbf{r}, t) \equiv \int_0^1 \mathrm{d}z N(\mathbf{r}, z, t), \quad (8)$$

and after integrating over z, neglecting surface effects ($S = 0$), and using expressions (4)–(8) in Eqs. (1)–(3), we get

$$l_T^2\nabla_T^2\Phi(r, t) - \tau\partial\Phi(\mathbf{r}, t)/\partial t - \Phi(\mathbf{r}, t) = -I_{\text{in}}(\mathbf{r}, t)A[\Phi(\mathbf{r}, t)], \quad (9)$$

with

$$A[\Phi(\mathbf{r}, t)] = 1/\{1 + f\sin^2[\Phi(\mathbf{r}, t) - \Phi_0]\} \quad \text{(Airy function)}$$

$$I_{\text{in}}(\mathbf{r}, t) = -4\mathcal{F}[1 - \exp(-\alpha L)][(1 - R_F)(1 + R_B)] \times |F_{\text{in}}|^2/\alpha L(1 - R_\alpha)^2,$$

$$R_\alpha = (R_F R_B)^{1/2}\exp(-\alpha L),$$

$$f = 4R_\alpha/(1 - R_\alpha)^2.$$

Equation (9) is the starting point, and the concentration will be on obtaining a solution at the beam center, where the switching is most relevant. To deal with arrays it is convenient to transform Eq. (9) into an integral equation by using the corresponding Green function (see Appendix A) given by

$$G(\mathbf{r} - \mathbf{r}', t - t') = \exp[-(\mathbf{r} - \mathbf{r}')^2/4(t - t')] \times \{\exp[-(t - t')]\}/4\pi(t - t'), \quad (10)$$

in which the space variables are scaled to l_D and t is scaled to τ as it follows naturally from Eq. (9); this scaling is kept throughout. The formal solution then reads as

$$\Phi(\mathbf{r}, t) = \Phi(\mathbf{r}, -\infty) + \int_{-\infty}^{t} \mathrm{d}t' \int_{\mathbf{r}'} \mathrm{d}^2\mathbf{r}' G(\mathbf{r} - \mathbf{r}', t - t') \times I_{\text{in}}(\mathbf{r}', t')A[\Phi(\mathbf{r}', t')]. \quad (11)$$

For N beams,

$$I_{\text{in}}(\mathbf{r}, t) = \sum_{j=1}^{N} I_j(t)\exp[-(\mathbf{r} - \mathbf{r}_j)^2/W^2],$$
$$W \equiv w/l_D, \quad (12)$$

where $\mathbf{r}_j$ is the position of the center of the jth beam. On substitution of Eq. (12) into Eq. (11) we can ignore the variation[9] of $\Phi(\mathbf{r}, t)$ over the spatial integration if $W < 1$ or $W \to \infty$ (plane-wave approximation). If we take $W < 1$—which in fact corresponds to the experimental situation—we can replace $\Phi(\mathbf{r}, t)$ by $\Phi(\mathbf{r}_j, t) \equiv \Phi_j(t)$ in Eq. (11). Using Eqs. (10) and (12) in Eq. (11) and assuming that $\Phi(\mathbf{r}, -\infty) = 0$, we obtain

$$\Phi_i(t) = \int_{-\infty}^{t} \mathrm{d}t' \int_{\mathbf{r}'} \mathrm{d}^2\mathbf{r}' G(\mathbf{r}_i - \mathbf{r}', t - t') \times \sum_{j=1}^{N} I_j(t')\exp[-(\mathbf{r}' - \mathbf{r}_j)^2/W^2]A_j(t') \quad (i = 1, 2, \ldots N), \quad (13)$$

where $A_j(t') \equiv \mathrm{A}[\Phi_j(t')]$. Integration over space variables leads to the following system of integral equations:

$$\Phi_i(t) = \int_{-\infty}^{t} \mathrm{d}t' \sum_{j=1}^{N} A_j(t')I_j(t')W^2 \times (\exp\{-d_{ij}^2/[W^2 + 4(t - t')] - (t - t')\}/[W^2 + 4(t - t')]) \quad (i = 1, 2, \ldots, N), \quad (14)$$

where $d_{ij}^2 \equiv (\mathbf{r}_i - \mathbf{r}_j)^2$.

In the steady state each Φ_i is constant in time; thus from Eq. (14)

$$\Phi_i = \sum_{j=1}^{N} A_j I_j M(d_{ij}) \qquad i = 1, 2, \ldots, N, \quad (15)$$

with $M(d_{ij})$ being the coupling coefficient:

$$M(d_{ij}) \equiv (W^2/4)\exp(W^2/4)\int_{W^2/4}^{\infty} \mathrm{d}u\, \exp(-d_{ij}^2/u - u)/u. \quad (16)$$

If $N = 1$, then $d_{ij} \equiv 0$, and we can explore the dependence of the switching power on the spot size

$$\Phi = A(\Phi)P\exp(W^2/4)E_i(W^2/4),$$

where $P \equiv IW^2/4$ is the scaled power and E_i is the exponential integral; then the switching power is such that

$$P_s \propto \exp(-W^2/4)/E_i(W^2/4). \quad (17)$$

Because $E_i \to \infty$ as $W \to 0$, the switching power decreases with spot size, as shown in Fig. 4. These results agree with those previously found both theoretically[7] and experimentally.[5] In the opposite limit, namely, $W \to \infty$, from expression (17), $P_s \propto W^2$ and thus the plane-wave limit is regained.

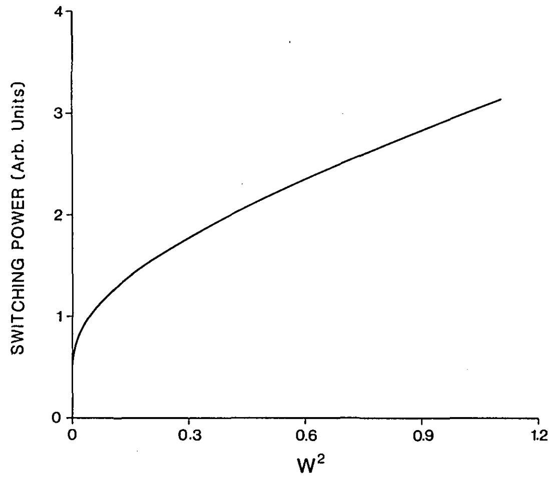

Fig. 4. Plot of switching power as a function of W^2 ($=W^2/l_D$) according to expression (17).

To work out the critical separation between elements we take two elements, E1 and E2, both with identical individual bistable characteristics and holding intensities I_{hold}. Then we assume that both elements are initially in the OFF state. Then E1 is suddenly switched on, and therefore the local-carrier concentration increases. As a result, diffusion from E1 into E2 occurs, which effectively changes the detuning of E2 and, with it, the bistable characteristic. Consequently the switching intensity I_s of E2 changes to a new[3] value $I_s' < I_s$ such that if $d_{12} > d_{\text{crit}}$, $I_s' > I_{\text{hold}}$, and E2 stays off; if $d_{12} < d_{\text{crit}}$ it follows that $I_s' < I_{\text{hold}}$, and E2 switches on. However, if $d_{12} = d_{\text{crit}}$, then $I_s' = I_{\text{hold}}$, and this defines d_{crit} from the relation

$$\partial I_2/\partial \Phi_2|_{I_2 = I_{\text{hold}}} = 0, \tag{18}$$

as explained below. Equation (18) is widely used to work out threshold parameters of bistable loops.

We can extend the above idea to a two-dimensional array by forming a square lattice for which we try to find the smallest lattice constant d such that the most unfavorably placed element EM—the one approximately in the middle—can sustain itself in the OFF state while all the others are on. Then, if EM is the mth element, the equivalent condition to Eq. (18) is

$$\partial I_m/\partial \Phi_m|_{I_m = I_{\text{hold}}} = 0, \tag{19}$$

which can be worked out by reexpressing Eq. (15) as

$$\Phi_m = A(\Phi_m)I_mM(0) + \sum_{j=1}^{N} A(\Phi_j)I_jM(d_{jm})(1 - \delta_{jm}), \tag{20}$$

where δ_{jm} is Kronecker's delta. Similar equations should in principle be added on for the remaining $N - 1$ phases. However, one can approximate Φ_j to a value Φ_{up} for every $j \neq m$ since the smaller slope of the upper branch prevents appreciable changes of the Φ_j's owing to changes in Φ_m. This fact was confirmed by the numerical simulations using Eq. (15); a similar effect occurs with the temperature in interference filters.[2] With this assumption we can apply Eq. (19) to Eq. (20) to obtain

$$I_{\text{hold}}M(0)f \sin 2(\Phi_c - \Phi_0)A^2(\Phi_c) + 1 = 0, \tag{21}$$

where Φ_c is the value of Φ_m at the switch-up point. Once we have solved for Φ_c in Eq. (21), substitution into Eq. (20) yields

$$\Phi_c = A(\Phi_c)I_{\text{hold}}M(0) + A(\Phi_{\text{up}})I_{\text{hold}} \sum_{j=1}^{N} (1 - \delta_{jm})M(d_{\text{crit}}\rho_{jm}), \tag{22}$$

where $\rho_{jm} \equiv d_{jm}/d_{\text{crit}}$; ρ_{jm} is a factor that depends on the relative position of the elements; for example, for two beams $\rho_{12} = 1$. Using Eq. (16) in Eq. (22), we can find the critical lattice constant d_{crit}. Figure 2(b) shows very good agreement between the prediction of Eq. (22) for two elements and the experiments when the corresponding parameters are used. The numerical solution of Eq. (14) agrees with the observed time delays, as shown in Fig. 3.

4. DISCUSSION

The present study of bistable cross talk differs from earlier work[10,11] on the transphasor type in which single-valued transfer curves with a region of large differential gain were used. Large element separations ($\sim$5 l_D) were required for near-independent operation, as any photogenerated carriers induced by, for example, E1, would continually diffuse to E2. However, between bistable elements there exists a logic cross talk in that the device will either be induced to switch or not with effectively no intermediate steady state. Moreover, as explained in Section 3, the diffused carriers from E1 have to produce a significant detuning in E2 to reduce the threshold below the holding power in order for it to switch. This result depends on the initial ΔP. We can then expect smaller separations than those of transphasor arrays. For example, from Fig. 2(a), if $\Delta P = 7\%$, then $d_{\text{crit}} \sim 160$ μm, which would allow a packing density of 4×10^3 cm^{-2}.

Time delays t_s ranging from 1 to 4 μsec were measured. For a fixed ΔP, t_s increased as d approached d_{crit} from below, and we can expect $t_s \to \infty$ as $d \to d_{\text{crit}}$ since for $d > d_{\text{crit}}$, by definition, there is no switching. The divergence of the time delay is attributed to critical slowing down,[12] which occurs as the threshold power P_s' (corresponding to I_s' defined in Section 3) approaches P_{hold} from below. In the standard critical slowing-down experiments through stepwise excitation, $P_{\text{hold}} \to P_s$, showing a symmetry with respect to our experiment. This effect was also found in the numerical integration[13] of Eq. (14) for two elements. A comparison between theory and experiment is shown in Fig. 3(d). To integrate Eq. (14) we assumed that both elements were initially in a steady state given by the solution of Eq. (15). Then an addressing pulse switches E1, which in turn switches E2 through cross talk at some time t_s later that depends on how close d is to d_{crit}. In Fig. 3(d) the observed time delay is plotted for $d = 165$ μm as the fraction I_{hold}/I_s is changed together with the corresponding predictions of the theory.

The effects of spot size, detuning, and finesse on d_{crit} for two elements were studied numerically. In Fig. 5(a) the variation of d_{crit} against I_{hold}/I_s for various values of w/l_D is shown. As expected, d_{crit}/w increases as w is decreased since the intensity increases[8] (and with it the carrier-concentration gradient) and therefore relatively more diffusion occurs.

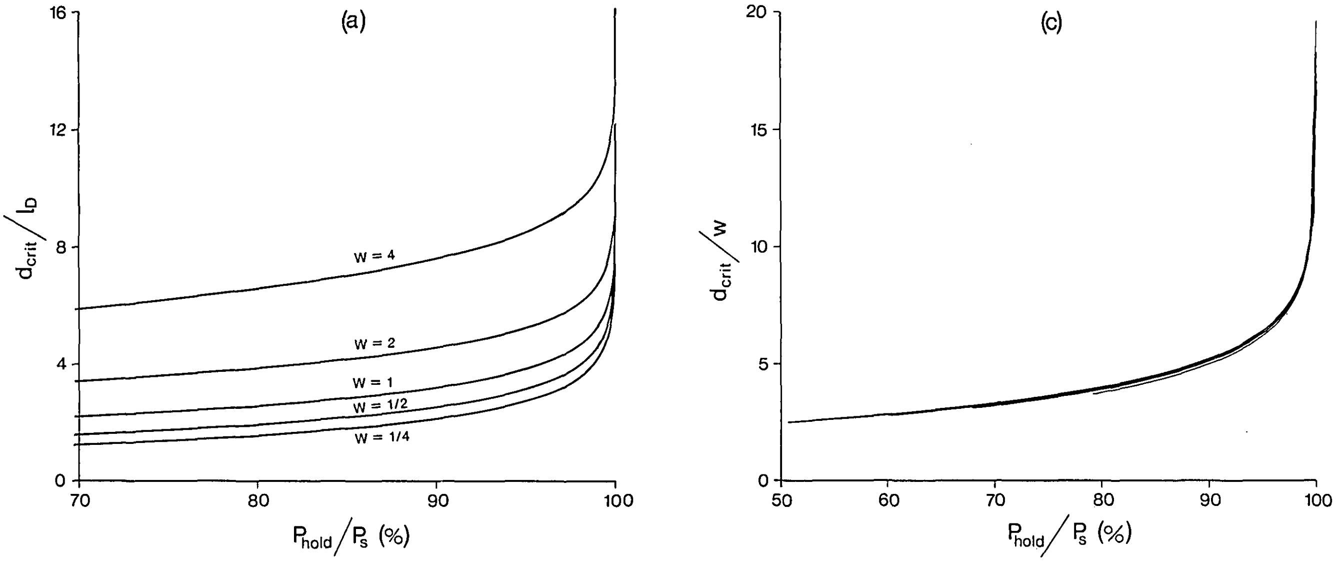

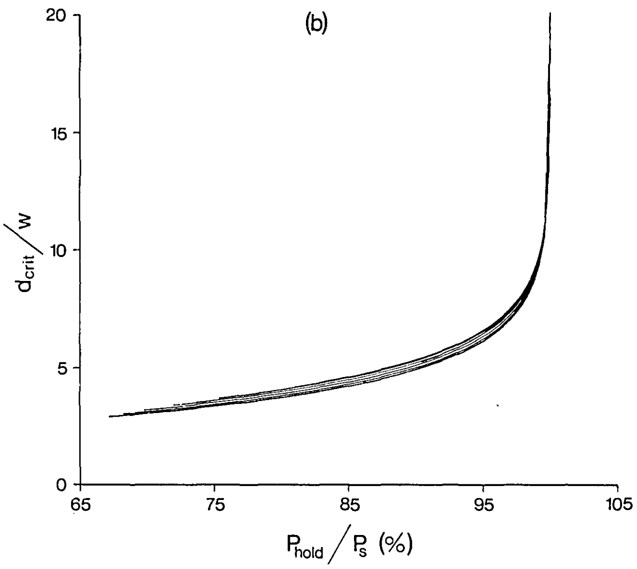

Fig. 5. Plot of critical distance as a function of P_{hold}/P_s according to Eq. (22): (a) for w/l_D = 0.25, 0.5, 1, 2, 4, in the upward direction; note that as w increases, d_{crit}/w decreases for a given holding intensity. Here f = 3.5 and $\Phi_0 = 0$. (b) The same plot for $0 \leq \Phi_0 \leq \pi$, f = 3.5, and w/l_D = 0.5. (c) The same plot for $2 \leq f \leq 128$, and w/l_D = 0.5, and Φ_0 = 0. In all cases the bistable mode of operation was ensured.

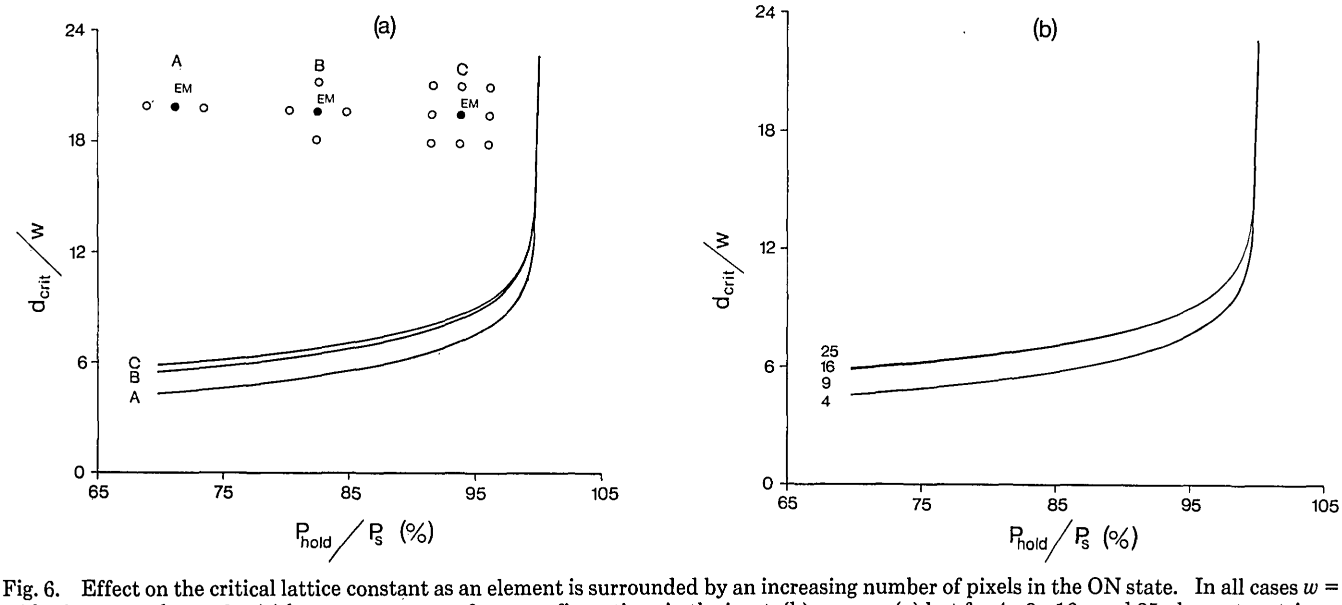

Fig. 6. Effect on the critical lattice constant as an element is surrounded by an increasing number of pixels in the ON state. In all cases $w = 0.5l_D$, f = 3.5, and $\Phi_0 = 0$: (a) letters on curves refer to configurations in the inset; (b) same as (a) but for 4-, 9-, 16-, and 25-element matrices.

Figures 5(b) and 5(c) show slight variations with detuning and finesse, respectively.

In Fig. 6(a) a simulation is shown of the effect of surrounding EM by two (A), four (nearest neighbors) (B), and eight (four nearest neighbors, four next-nearest neighbors) (C) elements on a square lattice. In going from two to four elements the difference is apparent, but when the next-nearest neighbors are added on, the critical lattice constant d_{crit} changes negligibly. This observation confirms previous findings[9] through heuristic arguments that, in systems with carrier diffusion as the transverse coupling mechanism, the interaction is limited to nearest neighbors. In Fig. 6(b) these calculations are extended to up to 25 elements with a barely noticeable difference, in sharp contrast to interference filters, which have a long-range coupling through thermal diffusion.

5. CONCLUSIONS

In this paper bistable cross talk between elements on an InSb Fabry–Perot êtalon was studied. The minimum separation for independent operation increases with the diffusion length, thus limiting the packing density of elements. This latter aspect, however, could be improved further by combinations of the following. First, the element's size can be decreased. However, as the numerical simulations of the present work imply, the carrier profile does not decrease proportionally. Second, it is not mandatory to use pure bulk InSb. If a large number of impurities were introduced they would reduce the carrier lifetime and thus the diffusion length, but the power requirements would be greater. Another possibility would be actual material pixellation by etching one surface of the êtalon to give a grid structure.

An important figure of merit in optical computing is the data-processing rate, defined as the product between packing density and switching rate (bits $\sec^{-1}$ cm^{-2}). The present switching rate for dispersive optical bistability in high-purity InSb is $\sim 10^6 \sec^{-1}$, which, with a packing density of 10^3 cm^{-2}, would give a data rate of $\sim 10^9$ bits $\sec^{-1}$ cm^{-2}. Pixellation of the sample and reduction of the element's size may stretch packing densities to up to 10^5 cm^{-2}, and, with increasing speeds due to impurity doping, data rates of 10^{13} bits $\sec^{-1}$ cm^{-2} may be possible. The observed optical delays in the microsecond region are required in some applications. Conventional methods of producing them, such as long path lengths, are bulky and often distort the beam. The present experiments suggest a compact technique to produce such delays. Finally, by choosing the appropriate separations, controllable cross talk could be used to perform logic functions in future computer architectures.

APPENDIX A

To obtain Green's function for this problem a particular solution of

$$-\nabla^2 G(\mathbf{r}-\mathbf{r}', t-t') + \partial G(\mathbf{r}-\mathbf{r}', t-t')/\partial t + G(\mathbf{r}-\mathbf{r}', t-t') = \delta(\mathbf{r}-\mathbf{r}', t-t') \quad \text{(A1)}$$

has to be found, where the spatial coordinates lie in the x–y plane and G is Green's function with a Fourier transform $\tilde{G}(\mathbf{k}, \omega)$ such that

$$G(\mathbf{r}-\mathbf{r}', t-t') = \int\int_{-\infty}^{\infty}\int \mathrm{d}^2\mathbf{k}\mathrm{d}\omega \tilde{G}(\mathbf{k}, \omega) \times \exp[i\mathbf{k}\cdot(\mathbf{r}-\mathbf{r}') + i\omega(t-t')]. \quad \text{(A2)}$$

Then on substitution of Eq. (A2) into Eq. (A1) and using the Fourier transforms of the delta functions,

$$\tilde{G}(\mathbf{k}, \omega) = -i/(2\pi)^{3/2}[\omega - i(k^2+1)]. \quad \text{(A3)}$$

By using Eq. (A3) in Eq. (A2), the integral over ω,

$$f(k) = \int_{-\infty}^{\infty} d\omega \exp[i\omega(t-t')]/[\omega - i(k^2+1)], \quad \text{(A4)}$$

can be solved exactly in the complex plane, yielding

$$f(k) = 2\pi i \exp[-(k^2+1)(t-t')],$$

and consequently

$$\begin{aligned} G(\mathbf{r} - \mathbf{r}, t-t') &= \exp[-(t-t') - (\mathbf{r}-\mathbf{r})^2/4(t-t')](2\pi)^{-2}\int\int_{-\infty}^{\infty} \mathrm{d}k_x \mathrm{d}k_y \\ &\times \exp\{-[k_x(t-t')^{1/2} - i(x-x')/2(t-t')^{1/2}]^2\} \\ &\times \exp\{-[k_y(t-t')^{1/2} - i(y-y')/2(t-t')^{1/2}]^2\}. \end{aligned}$$

Finally,

$$G(\mathbf{r}-\mathbf{r}', t-t') = \frac{\exp\{-(t-t') - [(\mathbf{r}-\mathbf{r}')^2/4](t-t')\}}{4\pi(t-t')}.$$

REFERENCES

1. S. D. Smith, I. Janossy, H. A. MacKenzie, J. G. H. Mathew, J. J. E. Reid, M. R. Taghizadeh, F. A. P. Tooley, and A. C. Walker, "Nonlinear optical circuit elements as logic gates for optical computers: the first optical digital circuits," Opt. Eng. **24,** 569 (1985).
2. E. Abraham, "Critical interpixel separation in nonlinear interference filters," Opt. Lett. **11,** 689 (1986).
3. E. Abraham and C. Rae, "Cross talk in nonlinear interference filters: loop narrowing and critical slowing down," J. Opt. Soc. Am. B **4,** 490 (1987).
4. D. J. Hagan, H. A. MacKenzie, H. A. Al-Attar, and W. J. Firth, "Carrier diffusion measurements in InSb by the angular dependence of degenerate four-wave mixing," Opt. Lett. **10,** 187 (1985).
5. D. J. Hagan, H. A. MacKenzie, J. J. E. Reid, A. C. Walker, and F. A. P. Tooley, "Spot size dependence of switching power for an optically bistable InSb element," Appl. Phys. Lett. **47,** 203 (1985).
6. E. M. Wright, W. J. Firth, and I. Galbraith, "Beam propagation in a medium with a diffusive Kerr-type nonlinearity," J. Opt. Soc. Am. B **2,** 383 (1985).
7. W. J. Firth, I. Galbraith, and E. M. Wright, "Diffusion and diffraction in dispersive optical bistability," J. Opt. Soc. Am. B **2,** 1005 (1985).
8. E. Abraham and W. J. Firth, "Periodic oscillations and chaos in a Fabry–Perot cavity containing a nonlinearity of finite response time," Opt. Acta **30,** 1541 (1983).
9. H. Richardson, E. Abraham, and W. J. Firth, "Modelling of cross talk in 2D bistable arrays with carrier diffusion," Opt. Commun. **63,** 199 (1987).
10. D. J. Hagan, I. Galbraith, H. A. MacKenzie, W. J. Firth, A. C. Walker, J. Young, and S. D. Smith, "Measurements of transverse coupling between adjacent InSb optical switching ele-

ments," in *Optical Bistability III*, H. M. Gibbs, P. Mandel, N. Peyghambarian, and S. D. Smith, eds. (Springer-Verlag, Berlin, 1986), p. 189.
11. D. J. Hagan, J. Young, and H. A. MacKenzie, "Diffusive transverse coupling between adjacent InSb transphasor channels," Opt. Lett. **12**, 696 (1987).
12. H. A. Al-Attar, H. A. MacKenzie, and W. J. Firth, "Critical slowing down phenomena in an InSb optically bistable étalon," J. Opt. Soc. B **3**, 1157 (1986).
13. H. J. J. te Riele, "Collocation methods for weakly-singular second kind Volterra equations with non-smooth solutions," IMA J. Numer. Anal. **2**, 437 (1982).